

REPORT DOCUMENTATION PAGE

Form Approved
OMB No. 0704-0188

Public reporting burden for this collection of information is estimated to average 1 hour per response, including the time for reviewing instructions, searching existing data sources, gathering and maintaining the data needed, and completing and reviewing this collection of information. Send comments regarding this burden estimate or any other aspect of this collection of information, including suggestions for reducing this burden to Department of Defense, Washington Headquarters Services, Directorate for Information Operations and Reports (0704-0188), 1215 Jefferson Davis Highway, Suite 1204, Arlington, VA 22202-4302. Respondents should be aware that notwithstanding any other provision of law, no person shall be subject to any penalty for failing to comply with a collection of information if it does not display a currently valid OMB control number. PLEASE DO NOT RETURN YOUR FORM TO THE ABOVE ADDRESS.

1. REPORT DATE (DD-MM-YYYY)

2. REPORT TYPE

Technical Papers

3. DATES COVERED (From - To)

4. TITLE AND SUBTITLE

5a. CONTRACT NUMBER

N/A

5b. GRANT NUMBER

5c. PROGRAM ELEMENT NUMBER

6. AUTHOR(S)

5d. PROJECT NUMBER

2308

5e. TASK NUMBER

M19B

5f. WORK UNIT NUMBER

7. PERFORMING ORGANIZATION NAME(S) AND ADDRESS(ES)

Air Force Research Laboratory (AFMC)
AFRL/PRS
5 Pollux Drive
Edwards AFB CA 93524-7048

8. PERFORMING ORGANIZATION
REPORT

9. SPONSORING / MONITORING AGENCY NAME(S) AND ADDRESS(ES)

Air Force Research Laboratory (AFMC)
AFRL/PRS
5 Pollux Drive
Edwards AFB CA 93524-7048

10. SPONSOR/MONITOR'S
ACRONYM(S)

11. SPONSOR/MONITOR'S
NUMBER(S)

12. DISTRIBUTION / AVAILABILITY STATEMENT

Approved for public release; distribution unlimited.

13. SUPPLEMENTARY NOTES

14. ABSTRACT

20030110 069

15. SUBJECT TERMS

16. SECURITY CLASSIFICATION OF:

17. LIMITATION
OF ABSTRACT

18. NUMBER
OF PAGES

19a. NAME OF RESPONSIBLE
PERSON

Leilani Richardson

19b. TELEPHONE NUMBER

(include area code)
(661) 275-5015

a. REPORT

b. ABSTRACT

c. THIS PAGE

Unclassified

Unclassified

Unclassified

A

Standard Form 298 (Rev. 8-98)
Prescribed by ANSI Std. Z39.18

21 separate items enclosed

2308M19B

MEMORANDUM FOR PR (Contractor/In-House Publication)

FROM: PROI (TI) (STINFO)

28 Jun 2000

SUBJECT: Authorization for Release of Technical Information, Control Number: **AFRL-PR-ED-TP-2000-143**
M. Braunstein (Spectral Sciences, Inc.); I. Wysong, "Direct Simulation Monte Carlo Modeling of High Energy Chemistry in Molecular Beams: Chemistry Models and Flowfield Effects"

International Symposium Rarefied Gas Dynamics
(Sydney, Australia, 09-14 Jul 00)

(Statement A)
(Submission Deadline: 09 Jul 00)

1. This request has been reviewed by the Foreign Disclosure Office for: a.) appropriateness of distribution statement, b.) military/national critical technology, c.) export controls or distribution restrictions, d.) appropriateness for release to a foreign nation, and e.) technical sensitivity and/or economic sensitivity.

Comments: _____

Signature _____ Date _____

2. This request has been reviewed by the Public Affairs Office for: a.) appropriateness for public release and/or b) possible higher headquarters review.

Comments: _____

Signature _____ Date _____

3. This request has been reviewed by the STINFO for: a.) changes if approved as amended, b.) appropriateness of distribution statement, c.) military/national critical technology, d.) economic sensitivity, e.) parallel review completed if required, and f.) format and completion of meeting clearance form if required

Comments: _____

Signature _____ Date _____

4. This request has been reviewed by PR for: a.) technical accuracy, b.) appropriateness for audience, c.) appropriateness of distribution statement, d.) technical sensitivity and economic sensitivity, e.) military/national critical technology, and f.) data rights and patentability

Comments: _____

APPROVED/APPROVED AS AMENDED/DISAPPROVED

LESLIE S. PERKINS, Ph.D (Date)
Staff Scientist
Propulsion Directorate

Direct Simulation Monte Carlo Modeling of High Energy Chemistry in Molecular Beams: Chemistry Models and Flowfield Effects

M. Braunstein

*Spectral Sciences, Inc.
99 S. Bedford St., Burlington, MA, 01803, USA*

I. J. Wysong

*Air Force Research Laboratory
AFRL/PRSA, Edwards AFB, CA, 93524, USA*

I. Introduction

Underlying the many models for simulating chemistry in rarefied gas flows are the cross sections for fundamental chemical processes occurring at high energy and under non-equilibrium conditions. As a rule, these cross sections are not known and must be extrapolated from thermal equilibrium measurements often beyond their measured energy range and far from thermal equilibrium. Large errors in the derived reaction probability can occur which are reflected in uncertainties in chemically reacting flow results. The problem of extracting cross sections from measured thermal data becomes even more difficult when a detailed quantum state specific cross section description is needed. In this paper, benchmark state-to-state cross sections previously obtained on O+CO vibrational energy excitation and chemical exchange reaction provide an opportunity to check the validity of widely used models for computing reaction probabilities from measured equilibrium reaction rates. The benchmark cross sections are converted to reactions probabilities based on the variable hard sphere (VHS) model for the total collision cross section and compared to extrapolations based on thermal measurements. To illustrate the impact of the use of the proper state-specific cross section on the results of rarefied gas simulations, the benchmark cross sections are used in the DSMC modeling of a high energy pulsed (non-steady) crossed-molecular beam experiment (MBE). Results from these simulations show how uncertainties in the input reaction cross sections are reflected in the predicted excited state populations and infrared radiation signature of the product molecules. A fully three dimensional DSMC simulation including reactive chemistry, energy exchange and radiative decay processes is described and used in the modeling. In addition, it is shown how these DSMC simulations can be an important diagnostic tool, enabling a more accurate extraction of fundamental cross sections from MBE data and extending the range of such measurements.

The paper proceeds as follows. Section II briefly describes the benchmark computational chemistry methods and results for O + CO collisions. Section III compares these benchmark results to those obtained with a widely used DSMC cross section model, showing the limitations of the method when only thermal rate constant measurements at relatively low collision energy are available. Section IV describes the DSMC simulation of a molecular beam measurement of fast O atoms interacting with target CO molecules using as input the state-specific cross sections obtained in the benchmark calculations. Section V gives conclusions.

II. Benchmark Cross Sections

Although high energy, non-thermal atomic oxygen interactions with carbon monoxide are important for gas-gas interactions near spacecraft, and as a model for understanding atomic oxygen reactivity in general, knowledge of this chemistry is limited, and derives mainly from room temperature measurements. Recently, however, Upschulte and Caledonia¹ have measured the cross section for vibrational excitation of CO by fast O at a collision energy of 3.4 eV (8 km/s) by monitoring the infrared radiation of the relaxing CO. Although rotational structure was not resolved, their results show a high degree of vibrational excitation. Besides the measurements of Upschulte and Caledonia,¹ Green *et al.*² in a space experiment have measured excitation of CO by O at similar energies with higher resolution. Their work shows both extended vibrational and rotational excitation of CO to high levels. But fundamental questions remain about the excitation mechanism and highly accurate absolute values of the excitation cross sections are not available.

→ move to
next line
w/ unit
(SHIFT +
ENTER)

Computational chemistry methods and hardware have progressed substantially in the past few decades, so that first-principles (no adjustable parameters) calculations have been shown to produce accurate energies³ and cross sections for systems at least as large as O + CO.⁴ These calculations have two stages: quantum chemistry electronic structure calculations which compute the forces (potential energy surfaces) between the colliding reactants and chemical dynamics calculations which use the force calculations to compute rates and cross sections. Benchmark "exact" calculations of reaction rates and cross sections for O+CO were performed using the latest codes from the academic community. The GAMESS (General Atomic and Molecular Electronic Structure System) suite of electronic structure codes³ was used to determine the molecular energies (potential forces between reacting atoms) along the reaction path and quasi-classical trajectory (QCT) chemical dynamics codes⁵ were used to calculate relevant reaction rates, based on these potentials. A complete description of the methods and results are given in Ref. 4. The following is a synopsis of the important results.

At low energy, and in the thermal regime (300⁰-4000⁰ K, roughly up to 0.5 eV) there is generally good agreement between theoretical and experimental rates for the O + CO system.⁴ Figure 1a shows calculated vibrational excitation cross sections for CO($v=0$) as a function of collision energy from 0.5 to 4 eV. Calculations were done at 0.5 eV, 1.0 eV, 2.0 V, 3.0 eV, and 4.0 eV collision energy. The dashed curve shows the calculated $v=0 \rightarrow v'=1$ cross section. The solid curve shows the calculated weighted sum of cross sections: $v=0 \rightarrow 1 + 2(v=0 \rightarrow 2) + 3(v=0 \rightarrow 3) + \dots$. Also shown is the data point at 8 km/s (3.4 eV) from the fast O(³P) measurements of Upschulte and Caledonia.¹ These authors measured the infrared radiation from vibrationally excited CO resulting from O+CO collisions but were not able to separate contributions from individual vibrationally excited states of the CO product. By making an approximation for the vibrationally excited state lifetimes, they converted the measured total radiation to the weighted sum of vibrational excitation cross sections defined above. The theoretical results are about an order of magnitude above the experimental measurement, which is surprising since there was good agreement with the high temperature vibrational relaxation measurements. Figure 1b shows the calculated infrared emission spectra of the nascent distribution of excited CO at an O+CO collision energy of 3.4 eV. The resolution is 5 cm⁻¹ and only quantum transitions to the next lowest vibrational state are included. The labeled peaks are locations of band heads to different final vibrational levels of CO. Very high vibrational excitation is evident. The band heads arise from excitation to high j ($j=50-100$) R branches of vibrationally excited CO and make a distinctive spectral signature. Figure 1c shows the same calculated spectra but degraded in resolution to match the data of Upschulte and Caledonia¹ which are also shown. Because experimental spectra were obtained at pressures which correspond to ~5 collisions within the sensor field of view in order to achieve good signal to noise, a direct comparison is not possible. But the agreement suggests that the calculations are at least qualitatively correct.

→ move to
next
line

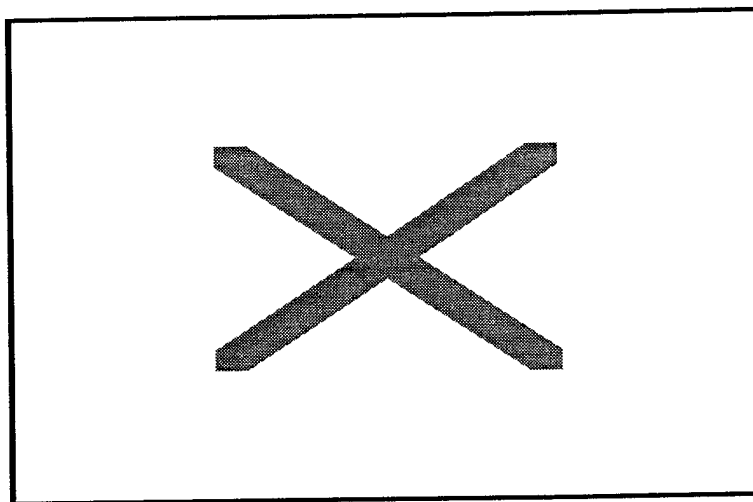


Figure 1. High energy vibrational excitation cross sections and spectra for O+CO collisions (a) cross sections (b) calculated high resolution spectra of the nascent products, (c) comparison of calculated (spectrally degraded) and experimental spectra.

III. Cross Section Models

Most of the available measurements on chemical reactions provide information in the form of rate coefficients. Rate coefficients inherently assume either full equilibrium or at least translational equilibrium at some temperature. The physics of individual collisions, however, is described by cross sections for processes as a function of translational energy, internal quantum states of the reactants and products, impact parameter, etc. DSMC can potentially reproduce reacting flowfields under conditions that are far from equilibrium (even translational equilibrium), but the technique requires incorporation of physically realistic cross sections.

The importance of proper characterization of high-energy cross sections is illustrated in Figure 2⁷ with calculations by Duff *et al.*⁶ for the reaction of $N(^4S) + O_2 \rightarrow NO + O$. First, it is noted that for the relatively low energy thermal region for which experimental data is available, the theoretically computed rate constant is in very reasonable agreement with the measured data. Typical collision energies for high-altitude interactions between surface and outgassing-species and atmospheric O for space contamination applications, for example, are typically in the 1 to 6 eV regime for which rate constants and/or cross sections are rarely available. The standard procedure, lacking such data, is to extrapolate the Arrhenius-fitted lower energy data to high energy. The perils of this approach are demonstrated in Figure 2b which shows that the extrapolated high energy cross sections underestimate the benchmark theoretical predictions obtained with computational chemistry tools by an order of magnitude in this case. While this particular reaction may not be of general relevance, it underscores the importance of establishing a reliable means of extending the more widely available thermal rate data into the higher energy regime.

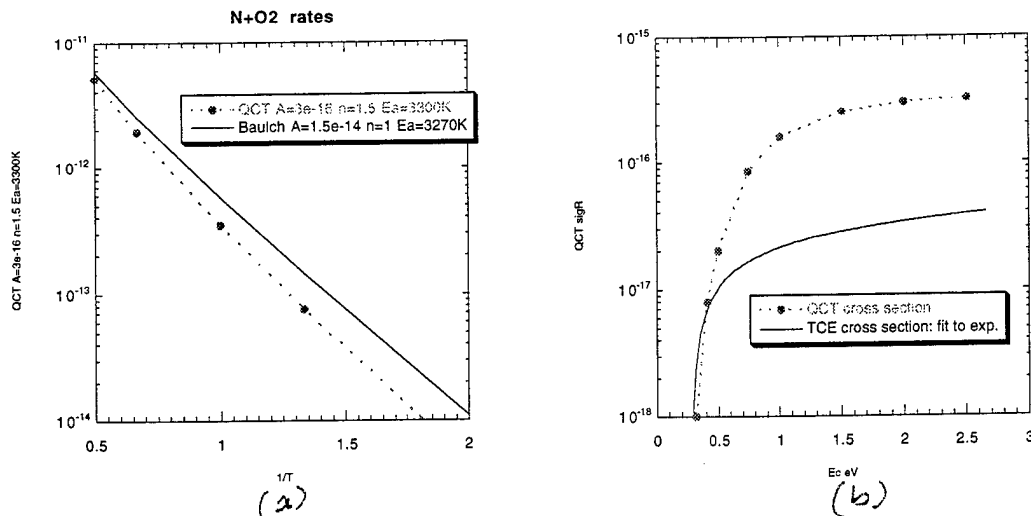


Figure 2. QCT rates from Ref. 5, along with experimental results for the reaction of $N + O_2 \rightarrow O + NO$. The left panel shows the thermal rates, and the right QCT and extrapolated energy specific cross sections.

The accurate state-to-state cross sections computed with the computational chemistry tools described above provide an opportunity to check the validity of widely used models for obtaining reaction probabilities from measured equilibrium reaction rate coefficients. A DSMC model for reaction probability as a function of the total collision energy that reproduces measured equilibrium reaction rates over a range of temperatures has been given by Bird.⁷ However, the role of the variable parameter (ζ) that represents the degrees of internal energy that contribute to the reaction probability is not well understood. Some sensitivity studies have been performed for this parameter.^{8,9}

For this study, we treat the ground and first excited vibrational levels of CO as separate chemical species, so that the collisional excitation process is treated as a chemical reaction: $O + CO(0) \rightarrow O + CO(1)$. This is motivated in part because a significant amount of vibrational excitation accompanies the chemical interaction of oxygen atom exchange. Figure 3 shows the thermal rate coefficient for this process obtained by QCT and the best fit using an Arrhenius expression. The parameters are: $A = 4.6e-13$ cm³/s, $n = 0.5$, $E_a = 0.465$ eV. Using these Arrhenius parameters, figure 4 shows the cross section that is obtained for $O + CO$ vibrational excitation using Eq. 6.8 from ref. 7. The assumed VHS values are: $\sigma_{ref} = 2.61e-15$ cm², $\omega = 0.75$, $T_{ref} = 2,000$ K. Note that a significant uncertainty with the comparison of the reaction cross section is associated with the uncertainty in the assumed VHS total collision cross section values. A change in these values by some factor would translate linearly into a change in predicted reaction cross section by the same factor.

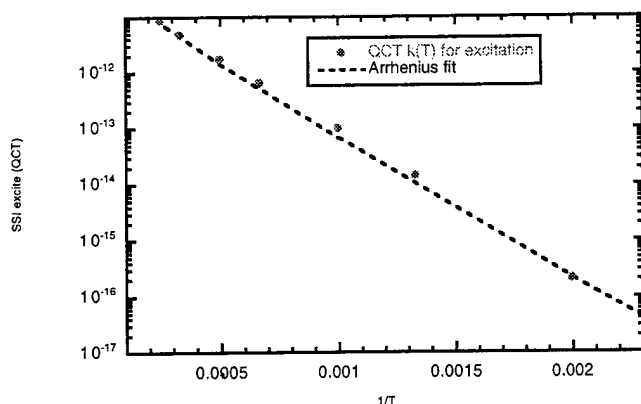


Figure 3. QCT and Arrhenius fit thermal rates for O + CO vibrational excitation.

The two curves in figure 4 represent the cases for $\zeta = 0$ and $\zeta = 1$. The $\zeta = 1$ value is the limit when CO rotational energy (in this case, internal energy is limited to rotational, since the vibrational levels are treated as species) contributes fully to the excitation process, while 0 is the limit where rotational energy does not contribute at all. While the two curves differ by less than a factor of two at higher energies, the difference is an order of magnitude at lower energies very close to the value of E_a . It can be seen that the $\zeta = 0$ case is much closer to the QCT cross sections, especially near the energetic threshold. This is initially surprising, since one might expect that rotational energy as well as translational energy would contribute to the excitation process.

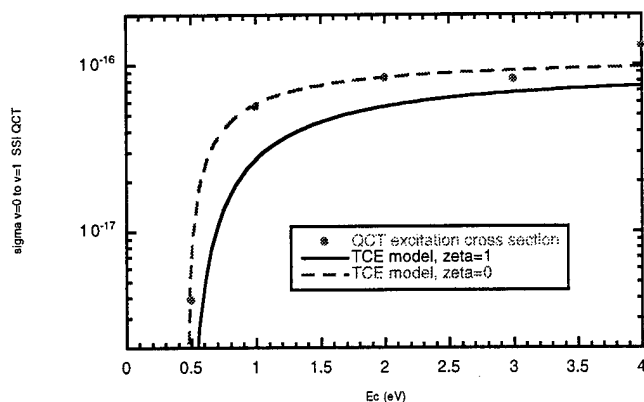


Figure 4. QCT and extrapolated cross sections for O + CO vibrational excitation.

This expectation would appear to be supported by the QCT results⁴ showing that, for collisional excitation at $E_{tr} = 3\text{eV}$, rotational and translational energy modes are populated nearly statistically in the product CO(1). However, specificity of energy consumption is not directly related to the specificity of product distribution, but rather to specificity of distribution in products of the reverse process. To assess the role of rotational energy in promoting CO vibrational excitation, figure (5) shows a plot of translational efficiency, defined:

$$|(\langle Et \rangle - \langle E_{ti} \rangle)| / (\langle Ev \rangle - \langle E_{vi} \rangle),$$

move to next line

for those trajectories achieving vibrational excitation, where $\text{CO}(v=0 \rightarrow 1)$. (Rotational energy efficiency is just defined as one minus the translational efficiency.) The QCT results for energy efficiency indicate that at low temperatures rotational energy is in fact not efficient in promoting the excitation process. Translational energy is nearly 100 % efficient at the lowest temperature and falls to about 70% efficiency at the highest temperatures. This, then, explains the fact that the model prediction for cross section based on QCT $k(T)$ and $\zeta = 0$ is much closer to the QCT cross section. Note, however, that the translational efficiency decreases for higher temperatures, reflecting the fact that a simple assumed constant value for ζ is an over-simplification.

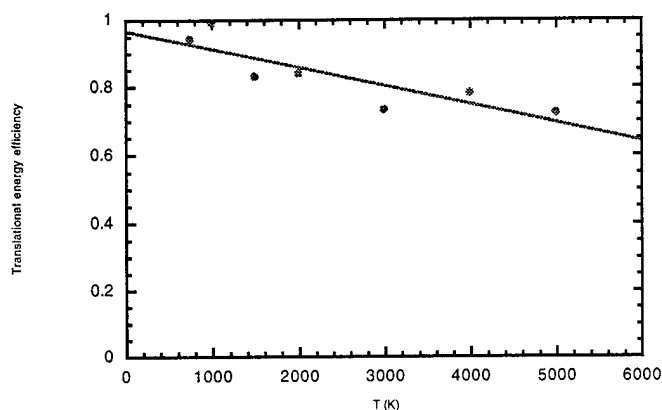


Figure 5. QCT results for translational energy efficiency as a function of temperature for $\text{O} + \text{CO}$ vibrational excitation.

Unfortunately, we have no guidance on how to choose the most reasonable value for ζ in the general case where the reaction dynamics are unknown. The uncertainty is exacerbated for the typical situation where "internal energy" may include both vibration and rotation. More work on this question would be very valuable. The difficulty in finding a reliable method for obtaining cross sections from rate coefficients underlines the valuable contribution that the increasing availability of computational chemistry tools will make.

IV. DSMC Modeling of Molecular Beams

In this section we use the state specific benchmark cross sections for $\text{O} + \text{CO}$ in a DSMC simulation with the SOCRATES (Spacecraft/Orbiter Contamination Representation Accounting for Transiently Emitted Species) computer code.^{10,11} SOCRATES was developed over ~15 years in a collaboration between the United States Air Force (AFRL, Hanscom, MA) and Spectral Sciences, Inc. (SSI). It is a three-dimensional DSMC code based on the original treatment of Bird⁷ and can treat steady, and non-steady (pulsed) flows, multiple interacting sources, non-equilibrium gas phase chemistry and infrared spectral emission from a wide variety of species. It can also treat solid bodies and model gas-surface interactions. Here it is applied to modeling the chemically reacting flow of a molecular beam experiment (MBE), and it is denoted as the molecular beam simulator (MBS).

We simulate the measurements described in Ref. 1 involving the interaction of high velocity ^{atomic oxygen} oxygen atoms with carbon monoxide. A diagram of this experiment is shown in Figure 6. A fast pulsed ~~O atom~~ (AO) beam intersects a much slower target beam of carbon monoxide (CO) and vibrationally excites the target molecules. The radiation from the decay of the collisionally excited CO is detected by the optical system, perpendicular to the plane of the O and CO sources. Knowledge of this optical signal level and the densities and fluxes of the AO and CO reactants leads to a determination of the cross section for excitation of the CO by AO at the relative collision velocity of the crossed beams (~8 km/s), the main result of the experiment. The principal uncertainty in the determination of the cross section in such an experiment derives from approximations of the number densities of the reactants in the

interaction region. By directly computing these number densities, the present DSMC simulations can remove much of this uncertainty.

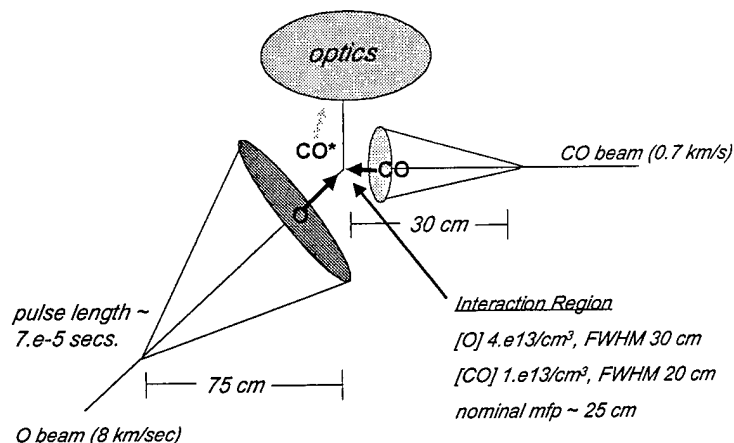


Figure 6. Diagram of pulsed, crossed beam apparatus for high velocity O + CO measurements of Ref. 1. The O and CO beams approach at right angles, produce collisionally excited CO which is detected by an optical system at right angles to the beam.

already defined

The fast ~~atomic oxygen~~ (AO) source and a slow CO target source in the crossed molecular beam laboratory experiment of Ref. 1 are modeled using the Brook far-field approximation¹⁰ for an isentropically expanding jet exhausting from a nozzle. Far-field approximations are very useful when the ratio of the distance from the source to the nozzle exit radius is large. The relevant source parameters and experimental setup are described in Ref. 1. The exit radius of the beam source nozzle is about 2.4 cm and the interaction region of the two crossing beams is 75 cm away from the AO source. We fit the experimentally determined number density profile of the ~~atomic oxygen (AO)~~ source by varying the parameters within the Brook model. The Brook model gives a good fit to the data for AO. For CO similar data is not available, but the correct fluxes, number densities and nominal widths are reproduced.

It is important to derive an analytic model which predicts the amount of radiation observed by the optical system assuming single-collision conditions in the molecular beam experiment. This analytic model should be consistent with the assumptions used in the determination of the excitation cross section from experimental observables. Differences between the DSMC results and the analytic model can then be traced to a breakdown of assumptions in the analytic model used to derive the cross section from experimental observables. These assumptions, can consist of the "single-collision" assumption, or a too simplified description of the source flows, for example. The number densities and other quantities found in the DSMC calculation can then be used to obtain a more accurate determination of the excitation cross section which is one of the main goals of this effort. Alternatively, the excitation cross section in the DSMC calculation can be varied to match the experimental observable.

Following Ref. 1, we develop an analytical expression for the collisional excitation cross section in terms of the experimentally observable (the number of photons/sec) and the number densities of O and CO in the interaction region. To reproduce these approximations in the derivation of the cross sections, we used the Brook source flow models described above. The number densities of O and CO are from Ref. 1, the cross section for excitation to $v=1$ is from Ref. 4, the pulse time of 9.375×10^{-5} seconds is slightly longer than the nominal 7×10^{-5} seconds of Ref. 1, and the relative velocity of 8×10^5 cm/second is a good approximation to the true collision velocity. When the excited number density is multiplied by the Einstein A coefficient and integrated over the area of the detector this is equal to the number of photons/sec, which is what is observed. The value for the pulse time, τ , is somewhat longer than the 7×10^{-5} seconds used in the experiment, but this should not affect very much the overall conclusions. The maximum line density of excited CO at the origin is $5.54 \times 10^{13} \text{ cm}^{-2}$. This "single-collision" value should be compared with the

keep on max line

molecular beam simulator results. Differences could point to a break-down in the single-collision assumption, or other assumptions, and inaccuracies in the cross sections derived in this way. *make subscript? or upper case T*

Figure 7 shows the time-sequence of pulsed (non-steady) runs used in the present DSMC calculations. In this perspective, the CO beam is turned on at $t=0$ seconds and is traveling below and through the page to the reader. The O atom beam leaves the source perpendicular to the CO beam at $t_1=1.44e-3$ seconds, and has a duration of $9.375e-5$ seconds. At t_2 , it starts to overlap the CO beam. At t_3 and t_4 it continues to overlap the CO beam, until finally at t_5 the O atom beam continues past the CO beam. After this time there will be few collisions between O and CO, and the flow will still be dominated by radiative decay of the collisionally excited CO molecules.

as in Fig. 7

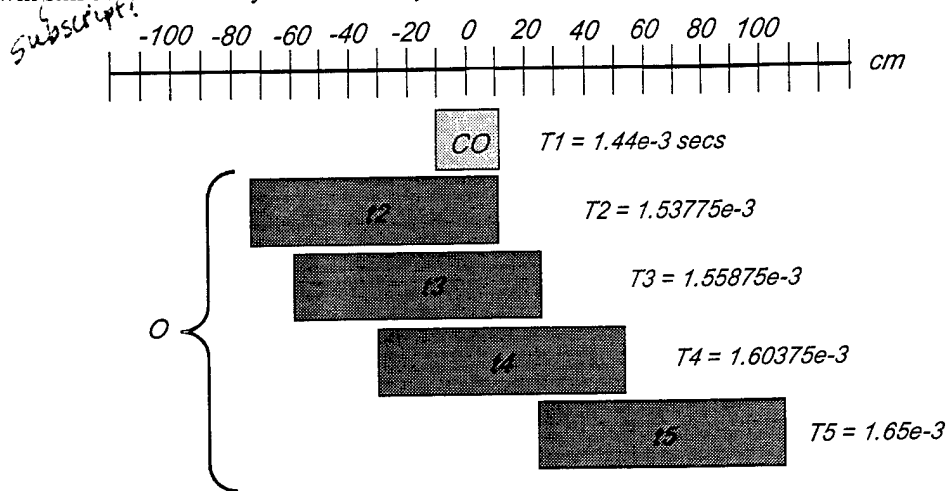


Figure 7. Time sequence of molecular beam simulation non-steady (pulsed) calculations.

Figure 8 shows the line integrated population of CO(1), the first excited vibrational state of CO which is one of the products of the O + CO collisions, in units of number per cm^2 at each step in the time sequence in the present DSMC calculations using the benchmark O + CO cross sections described above. These frames are proportional to what the detector perpendicular to the crossed beams would see. The source flows for O and CO, geometry and conditions, and cross sections are all consistent with the analytic model described above. The computational spatial grid used is fairly coarse, about ~ 15 cm resolution near the origin, for these computationally demanding calculations. As we would expect, as the O atom beam crosses the CO beam, starting at t_2 , the signal increases. By t_5 the AO beam has crossed the CO target beam and the collisionally excited molecules are beginning to spread out due to their final state velocity, and also they begin to radiatively decay. This population continues to move and decay from an initial maximum as time elapses until it moves out of the computational cube. The actual experimental measurements integrate over the detector area to boost signal and so cannot achieve any spatial resolution, but it would be interesting to compare the present spatial distributions as a function of time with future measurements which may be able to spatially and time resolve the signal.

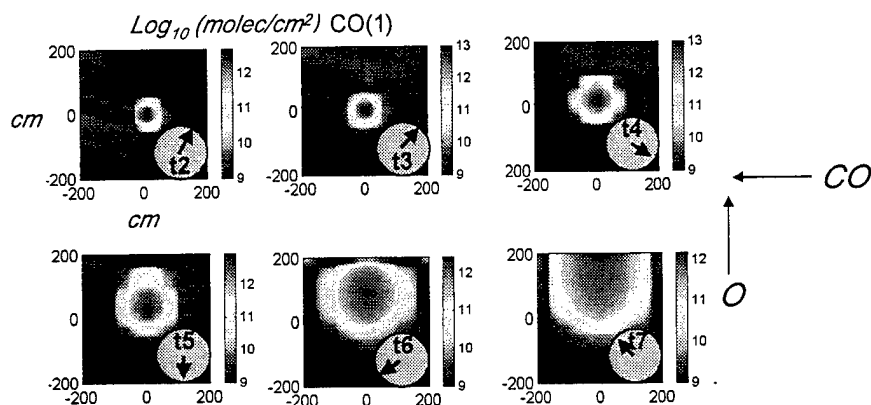


Figure 8. Line densities ($\log_{10} \text{ molec/cm}^2$) of CO(1) from the point of view of the detector as the O-atom beam passes through the interaction region.

Figure 9 shows the value of the line density at the origin of excited CO from the DSMC calculations as a function of time. The actual detector will integrate over a small area near the origin. But this should not make much of a difference, and our calculations are on a coarse grid and so this spatial integration will not have much meaning. The peak of the line density is between t_3 and t_4 , near where the O atom pulse has finished crossing the CO beam. By t_5 , after the O atom beam is past the CO target, the intensity continues to fall. Also shown is the value of the single-collision "analytic" result derived earlier. The DSMC peak is about a factor of 5 below the "analytic" result. This difference, we believe, comes from the multi-collision conditions in the flow, and can only be accounted for by a method like DSMC which goes beyond single collisions. The effects of multi-collisions tend to push away the available CO target molecules in the interaction region, and therefore decrease the number of excitation collisions from that expected from single-collision densities. This suggests that the actual measurements reported a lower bound to the cross section, which is consistent with the theoretical cross sections in Ref. 4. Calculations at lower AO fluxes show that these multi-collisions effects lessen considerably, and better agreement between the analytic model and MBS results are obtained.

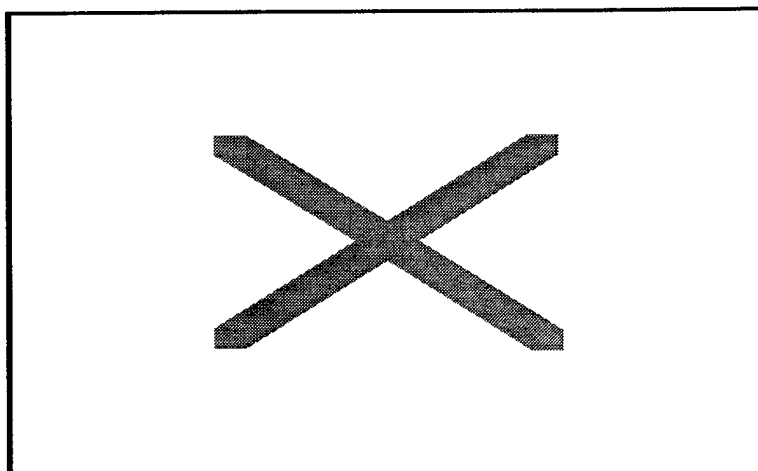


Figure 9. Comparison of analytic and molecular beam simulation results for O + CO crossed beam experiment. Line integrated intensities for CO(1) as a function of time.

To further illustrate this multi-collision effect, we show in Figure 10 the molecular beam simulator number densities in the plane of the O and CO crossed beams for time snapshots t_4 and t_5 . This is toward the end of the time when the O atom pulse crosses the CO beam. The flow of the CO beam appears to be changed from the undisturbed source toward the end of the O atom pulse. As sketched in Figure 11, the beginning of the O atom pulse pushes away some of the target CO molecules, so by the end of the pulse there is a decreased number density of target CO in the interaction region for the AO to interact with. These multi-collision effects manifest in a lower than expected

product population of vibrationally excited CO seen in the molecular beam simulator calculations. To check these results we have done calculations with the O source number densities a factor of 10 lower. This should decrease the multi-collision effects observed above. Indeed, the difference between the analytic result and the DSMC result decreases from a factor of 5 to a factor of 2 for the maximum line integrated number density of excited CO for these lower density calculations. In contrast to the higher density AO case shown in Figure 10, the CO target beam in this lower flux case seems almost completely undisturbed by the AO beam, which ultimately brings the observed signal closer to single-collision assumptions.

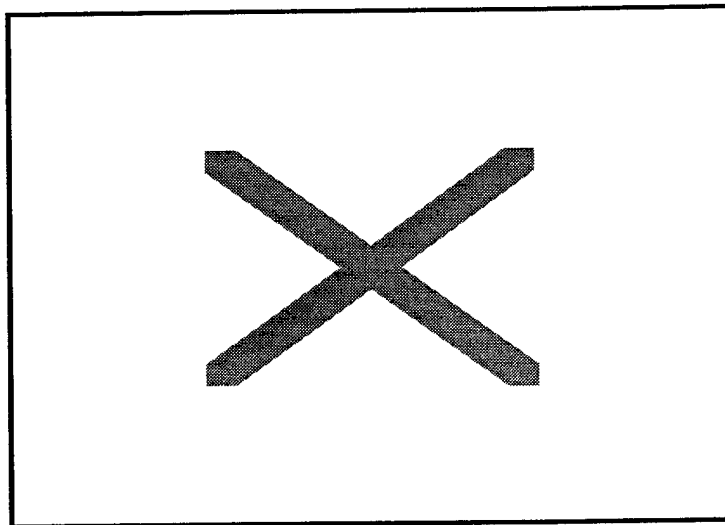


Figure 10. Time snapshots of reactant and product species in the plane of the two sources. Note the “turning” of the CO(0) right-to-left flow due to impingement of the high-flux [O] beam from below.

We note that if we use the model cross sections with $\zeta=1$, the vibrational excitation cross section would be less and so the signal levels would naturally be less than the benchmark cross sections. However, there would still be differences with the analytic model. A direct comparison with raw, experimentally observed signal levels would be helpful in understanding the relative value of these model cross section extrapolation errors.

The flow-field effects found here in modeling the fast O + CO molecular beam measurements are not conclusive. Uncertainties in the source modeling, the relatively coarse spatial grid, and uncertainties in the VHS cross section used could all lead to problems in modeling the exact conditions of the molecular beam experiment. We note that in calibrating their measurements, the authors of Ref. 1 confirmed linearity of the signal with increasing pressure. Measurements at other energies and at much lower pressures would be helpful in resolving these issues.

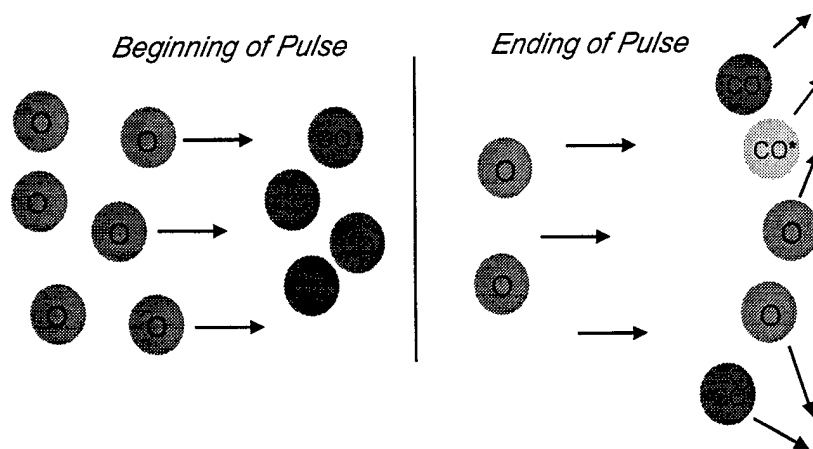


Figure 11. Multi-collision effects for the O + CO crossed beam experiment.

V. Conclusions

In this paper, benchmark state-to-state cross sections previously obtained on O+CO vibrational energy excitation are used to check the validity of widely used models for computing reaction probabilities from measured equilibrium reaction rates. The benchmark cross sections are converted to reactions probabilities based on the variable hard sphere (VHS) model for the total collision cross section and compared to extrapolations based on thermal measurements. To illustrate the impact of the use of the proper state-specific cross section on the results of rarefied gas simulations, the benchmark cross sections are used in the DSMC modeling of a high energy pulsed crossed-molecular beam experiment (MBE). Flow field effects change the expected reactant concentrations in the chamber leading to some uncertainty in the derived cross section. Experiments at much lower pressures would help elucidate these effects.

Acknowledgments

We are grateful to G. Caledonia and R. Krech of Physical Sciences, Inc. and L. Bernstein of Spectral Sciences, Inc. for several helpful discussions. The authors are also grateful to J. Duff of Spectral Sciences, Inc. for helpful discussions and aid in performing QCT calculations on the O + CO system. Grateful acknowledgment of a NASA Small Business Innovative Research (SBIR) grant which helped support part of this work is also made. IJW acknowledges support from the Air Force Office of Scientific Research, with Dr. Mitat Birkan as Technical Monitor.

References

1. Upschulte, B. L. and Caledonia, G. E., *J. Chem. Phys.* **96**, 2025 (1992).
2. Green, B. D., Holtzclaw, K. W., and Joshi, P. B. "Analysis of Radiances from Orbital Gas Releases", *J. of Geophysical Research*, **97**, 12,161-12,172 (1992).
3. Schmidt, M. W., Baldridge, K. K., Boatz, J. A., Elbert, S. T. Gordon, M. S. Jensen, J. H. Koseki, S., Matsunaga, N., Nguyen, K. A., Su, S. J., Windus, T. L., Dupuis, M., Montgomery, J. A., "The GAMESS Suite of Electronic Codes", *J. Comput. Chem.* **14**, 1347-1370, 1993.
4. Braunstein, M. and Duff, J. W., "Electronic Structure and Dynamics of O + CO Collisions", *J. Chem. Phys.* **112**, pp. 2736-2745 (2000).
5. Truhlar, D. G. and Muckerman, J. T., "Atom-Molecule Collision Theory", ed. R. B. Bernstein, Plenum Press, New York, p. 505 (1979).
6. Duff, J. W., Bien F., and Paulsen, D. E., *Geophys. Res. Lett* **21**, 2043 (1994).
7. Bird, G. A., *Molecular Gas Dynamics and the Direct Simulation of Gas Flows*, Clarendon Press, Oxford, 1994.
8. Bird, G. A., "Simulation of multi-dimensional and chemically reacting flows" in *Rarefied Gas Dynamics*, edited by R. Campargue., Proceedings of the Eleventh International Symposium, CEA, Paris, 1979, p. 365. *is this part of title?*
9. Boyd, I. D., *J. Thermophysics* **4**, 487 (1990).
10. Elgin, J. B. and L. S. Bernstein, "The Theory Behind the Socrates Code", Phillips Laboratory, Report PL-TR-92-2207, (August, 1992).
11. Elgin, J. B., Cooke, D. C., Tautz, M. F., Murad, E., "Modeling of Atmospherically Induced Gas Phase Optical Contamination from Orbiting Spacecraft," *J. of Geophysical Research*, **95**, 12197-12,208 (1990).

initial
caps on title